

## Vacuum ultraviolet photoionization of carbohydrates and nucleotides

Joong-Won Shin<sup>1</sup> and Elliot R. Bernstein<sup>1</sup>

Citation: *The Journal of Chemical Physics* **140**, 044330 (2014); doi: 10.1063/1.4862829

View online: <http://dx.doi.org/10.1063/1.4862829>

View Table of Contents: <http://aip.scitation.org/toc/jcp/140/4>

Published by the *American Institute of Physics*

---

---

**COMPLETELY**

**REDESIGNED!**



**PHYSICS  
TODAY**

*Physics Today* Buyer's Guide  
Search with a purpose.

# Vacuum ultraviolet photoionization of carbohydrates and nucleotides

Joong-Won Shin<sup>1,2,a</sup> and Elliot R. Bernstein<sup>2,b</sup>

<sup>1</sup>Division of Science, Governors State University, University Park, Illinois 60484-0975, USA

<sup>2</sup>Department of Chemistry, Colorado State University, Fort Collins, Colorado 80523-1872, USA

(Received 22 October 2013; accepted 8 January 2014; published online 31 January 2014)

Carbohydrates (2-deoxyribose, ribose, and xylose) and nucleotides (adenosine-, cytidine-, guanosine-, and uridine-5'-monophosphate) are generated in the gas phase, and ionized with vacuum ultraviolet photons (VUV, 118.2 nm). The observed time of flight mass spectra of the carbohydrate fragmentation are similar to those observed [J.-W. Shin, F. Dong, M. Grisham, J. J. Rocca, and E. R. Bernstein, *Chem. Phys. Lett.* **506**, 161 (2011)] for 46.9 nm photon ionization, but with more intensity in higher mass fragment ions. The tendency of carbohydrate ions to fragment extensively following ionization seemingly suggests that nucleic acids might undergo radiation damage as a result of carbohydrate, rather than nucleobase fragmentation. VUV photoionization of nucleotides (monophosphate-carbohydrate-nucleobase), however, shows that the carbohydrate-nucleobase bond is the primary fragmentation site for these species. Density functional theory (DFT) calculations indicate that the removed carbohydrate electrons by the 118.2 nm photons are associated with endocyclic C–C and C–O ring centered orbitals: loss of electron density in the ring bonds of the nascent ion can thus account for the observed fragmentation patterns following carbohydrate ionization. DFT calculations also indicate that electrons removed from nucleotides under these same conditions are associated with orbitals involved with the nucleobase-saccharide linkage electron density. The calculations give a general mechanism and explanation of the experimental results. © 2014 AIP Publishing LLC. [<http://dx.doi.org/10.1063/1.4862829>]

## I. INTRODUCTION

Photoionization of biological molecules often leads to extensive fragmentation of the molecular ions.<sup>1–9</sup> In particular, studies<sup>10–15</sup> strongly support the idea that radiation induced damage of DNA and RNA molecules can be accounted for by the fact that carbohydrates, which are constituents of the nucleic acid molecules, are highly susceptible to molecular fragmentation by high energy particles and radiation. The dominant carbohydrate ionization products are fragment ions only,<sup>8–17</sup> and intact molecular ions are rarely observed.

Our group has recently carried out an investigation<sup>8</sup> of extreme ultraviolet (EUV, 46.9 nm, 26.44 eV) ionization and fragmentation behavior of carbohydrate molecules in the gas phase. The study shows that carbohydrates undergo complete fragmentation upon photoionization at this energy, and unlike many biological molecules, the ion state behavior does not depend on their conformations despite the presence of a highly complex intramolecular hydrogen bonding network. A possible reason for this fragmentation behavior is that EUV photons ionize inner valence endocyclic C–C and C–O bonds, which are not involved in intramolecular hydrogen bonding interactions.

In the current study, we carry out photoionization mass spectrometry for the carbohydrates 2-deoxyribose, ribose, and xylose using vacuum ultraviolet (VUV, 118.2 nm, 10.49 eV) radiation to explore the possibility of conformation depen-

dent ionization, and the fragmentation patterns of these three molecules. The VUV photon energy is near the ionization threshold<sup>9</sup> of carbohydrates. Single photon ionization at 10.49 eV thus ensures that only the highest occupied molecular orbitals (HOMOs) for each carbohydrate, and those orbitals that are energetically close to these will be ionized. The experiment is extended to the nucleotides adenosine-, cytidine-, guanosine-, and uridine-5'-monophosphate to gain insight into the cause and mechanism of radiation damage of nucleic acids. By studying carbohydrates and nucleotides separately, one can, in principle, determine the component of DNA and RNA that is responsible for nucleic acid radiation sensitivity and ensuing damage. Chemically modified nucleotides have previously been generated<sup>18</sup> in the gas phase through laser desorption; however, to the best of our knowledge, the current study involves the first experiment in which unlabeled, isolated nucleotides are prepared in the gas phase through a similar technique. Density functional theory calculations are also employed for analysis of experimental findings.

## II. EXPERIMENTAL PROCEDURES

Carbohydrates 2-deoxy-D-ribose (C<sub>5</sub>H<sub>10</sub>O<sub>4</sub>), D-ribose, D-xylose, and D-1,2-<sup>13</sup>C<sub>2</sub>-xylose (pentoses, C<sub>5</sub>(H<sub>2</sub>O)<sub>5</sub>), and nucleotides adenosine-, cytidine-, guanosine-, and uridine-5'-monophosphate (A5MP [C<sub>10</sub>H<sub>14</sub>N<sub>5</sub>O<sub>7</sub>P], C5MP [C<sub>9</sub>H<sub>14</sub>N<sub>3</sub>O<sub>8</sub>P], G5MP [C<sub>10</sub>H<sub>12</sub>N<sub>5</sub>O<sub>8</sub>P], and U5MP [C<sub>9</sub>H<sub>11</sub>N<sub>2</sub>O<sub>9</sub>P]) are used in the experiments (at Colorado State University). 2-deoxyribose, ribose, xylose, C5MP,

<sup>a</sup>Electronic mail: [jshin@govst.edu](mailto:jshin@govst.edu). Tel.: (708) 235-2835. Fax: (708) 534-1641.

<sup>b</sup>Electronic mail: [erb@lamar.colostate.edu](mailto:erb@lamar.colostate.edu). Tel.: (970) 491-6347. Fax: (970) 491-1801.

and U5MP are purchased from Sigma-Aldrich, A5MP and G5MP are purchased from Alfa Aesar, and 1,2-<sup>13</sup>C<sub>2</sub>-xylose is purchased from Omicron Biochemicals. The nucleotides are stored in a dry ice container prior to use to prevent sample degradation. Each saccharide is mixed and ground with rhodamine 6G (R6G) matrix, and the powder mixture is applied on a tape attached on a drum. Due to small quantities available, each nucleotide sample is dissolved with the R6G matrix in a weakly acidic methanol solution, and the solution is sprayed onto the drum in the form of fine mist. The solvent is evaporated using a halogen lamp as the solution is being sprayed. A motor attached to the front of a Jordan Co. pulse valve rotates and translates the drum so that fresh sample powder is gently desorbed by each 532 nm laser pulse.<sup>19–23</sup> In particular, use of the R6G matrix has been demonstrated<sup>18–22</sup> to be a very effective approach for desorbing and vaporizing molecules without fragmentation. The desorbed sample is carried to the ionization region of a time of flight (TOF) mass spectrometer using supersonic expansion of He gas (40 psi backing pressure), and is collimated by a skimmer with the aperture diameter of 1 mm. The base pressure of the mass spectrometer is in the  $\sim 9 \times 10^{-8}$ – $1 \times 10^{-7}$  Torr range with the liquid N<sub>2</sub> cooled photoionization region.

Ionization of the jet cooled samples is carried out with VUV photons (118.2 nm, 10.49 eV). As described previously,<sup>3,24</sup> the ninth harmonic of the Nd:YAG fundamental (1064 nm) is generated through the excitation of Xe gas in a 1:10 Xe/Ar mixture using the third harmonic (355 nm) of the fundamental with the conversion efficiency of  $1.2 \times 10^{-5}$ .<sup>25</sup> A MgF<sub>2</sub> lens tightly focuses the VUV photons on the ionization spot, but diffuses the nearly collinear 355 nm. The energy of the VUV laser at the ionization spot ( $\sim 0.1$  mm) is  $\sim 1$   $\mu$ J/pulse ( $\sim 10^{12}$  photons/pulse in 10 ns): under these conditions, only single photon ionization can be expected.<sup>26,27</sup>

VUV ionization of laser desorbed pure R6G is also carried out to verify that all assigned peaks are ionization products of the samples and not of the matrix.

### III. COMPUTATIONAL METHODS

Calculations are performed using the GAUSSIAN 09 software package<sup>28</sup> (at Governors State University). Structure optimization and harmonic vibrational frequency analysis of carbohydrates are carried out at the X3LYP/6-311G(d,p) theory level, and those of nucleotides are carried out at the X3LYP/Gen level using 6-31G for C atoms and 6-31G(d) for H, N, O, and P atoms. Force constants are calculated for all initial geometries. The more commonly used B3LYP method is specifically avoided because it does not predict the observed cyclic carbohydrate structure ( $\beta$ -pyranose form) to be the global minimum.<sup>29</sup> A proper description of dispersion interaction is important for density functional theory studies of carbohydrate structures,<sup>29</sup> and the X3LYP extended hybrid method has been shown<sup>30</sup> to describe the interaction effectively.

Converged third order pole ionization energies of different molecular orbitals are calculated with the partial third

order electron propagator theory method<sup>31,32</sup> EPT = P3/6-311G(d,p) using structures optimized as described above.

## IV. RESULTS AND DISCUSSION

### A. VUV ionization of carbohydrates

The measured vertical ionization energy of 2-deoxyribose, the carbohydrate group in DNA, is in the 9.6–10 eV range,<sup>9</sup> which is near the VUV photon energy of 10.49 eV. Figure 1(a) presents 2-deoxyribose VUV ionization results, along with our previous EUV ionization result<sup>8</sup> shown in Figure 1(b) for comparison (data in Figure 1(b) are directly adopted from Ref. 8). Ionization using the two lasers yields similar fragment ions, with VUV ionization preferentially generating larger concentrations of the same high mass ions. No parent molecular ion is observed for EUV ionization: low mass ions are prevalent in the EUV mass spectrum, but some of these (e.g.,  $m/z = 16, 28, 44$ ) may well be background enhanced (O<sub>2</sub><sup>+</sup>, N<sub>2</sub><sup>+</sup>, or CO<sub>2</sub><sup>+</sup>). A similar pattern is also observed for protonated oligonucleotides,<sup>33</sup> which generate lower mass ions with increasing ionization energies as core orbitals are ionized. The observed ions in both mass spectra are assigned<sup>8</sup> as  $m/z = 18$  (H<sub>2</sub>O<sup>+</sup>), 19 (H<sub>3</sub>O<sup>+</sup>), 28 (CO<sup>+</sup> or C<sub>2</sub>H<sub>4</sub><sup>+</sup>), 29 (CHO<sup>+</sup>), 31 (CH<sub>3</sub>O<sup>+</sup>), 42 (C<sub>2</sub>H<sub>2</sub>O<sup>+</sup>), 43 (C<sub>2</sub>H<sub>3</sub>O<sup>+</sup>), 55 (C<sub>3</sub>H<sub>3</sub>O<sup>+</sup>), 56 (C<sub>3</sub>H<sub>4</sub>O<sup>+</sup>), 57 (C<sub>3</sub>H<sub>5</sub>O<sup>+</sup>), 60 (C<sub>2</sub>H<sub>4</sub>O<sub>2</sub><sup>+</sup>), 70 (C<sub>3</sub>H<sub>2</sub>O<sub>2</sub><sup>+</sup>), 73 (C<sub>3</sub>H<sub>5</sub>O<sub>2</sub><sup>+</sup>), 74 (C<sub>3</sub>H<sub>6</sub>O<sub>2</sub><sup>+</sup>), 75 (C<sub>3</sub>H<sub>7</sub>O<sub>2</sub><sup>+</sup>), 86 (C<sub>4</sub>H<sub>6</sub>O<sub>2</sub><sup>+</sup>), 88 (C<sub>4</sub>H<sub>8</sub>O<sub>2</sub><sup>+</sup>), 103 (C<sub>4</sub>H<sub>7</sub>O<sub>3</sub><sup>+</sup>), 116 (C<sub>5</sub>H<sub>8</sub>O<sub>3</sub><sup>+</sup>), and 134 (C<sub>5</sub>H<sub>10</sub>O<sub>4</sub><sup>+</sup>). The  $m/z = 116$  ion arises from a dehydration reaction (loss of H<sub>2</sub>O), and the  $m/z = 134$  ion is the parent molecular ion (dRb<sup>+</sup>), observed only by VUV ionization: all other fragments involve endocyclic C–C and C–O bond dissociation.

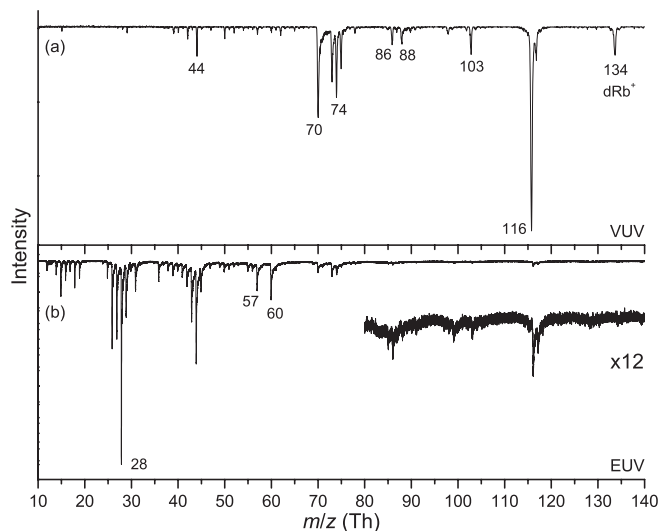


FIG. 1. TOF mass spectra of 2-deoxyribose mixed with a R6G matrix, ionized with (a) VUV and (b) EUV photons. Data presented in (b) are directly adopted from Ref. 8. Similar fragmentation patterns are observed. The molecular ion ( $m/z = 134$ ) is only observed from VUV ionization. Reprinted with permission from J.-W. Shin, F. Dong, M. E. Grisham, J. J. Rocca, and E. R. Bernstein, “Extreme ultraviolet photoionization of aldoses and ketoses,” Chem. Phys. Lett. **506**, 161–166 (2011). Copyright 2011 Elsevier.

EUV ionization can result in more extreme fragmentation than can VUV ionization, because EUV ionization can, in principle, leave more energy in the nascent ion than can VUV ionization. EUV ionization may remove an electron from much more strongly bonded orbitals: the excess photon energy following either ionization method is generally removed as photoelectron kinetic energy, as observed in photoelectron spectroscopy and laser ionization time of flight mass spectrometry studies.<sup>34–40</sup> The EUV created nascent ion, therefore, can potentially have more internal energy than the VUV created ion due to the ionization of deeper lying orbitals, in which electrons are bound with greater energies than in the outermost valence orbital. The ion can directly fragment from this state, relax to lower energy ion states  $D_i$ , or relax to the ground ion state  $D_0$ , and then use the created vibrational excitation to break chemical bonds. One can view this situation in the same manner as is relevant for the photochemistry of any organic molecule. The excited states are all coupled through conical intersections, and ultrafast internal, non-Born Oppenheimer vibronic dynamics can ensue to bring the highly excited ion through the various ion states,  $D_n$  to  $D_0$ , conserving energy, and following the minimum energy reaction coordinate.<sup>41–43</sup> Depending on the multidimensional potential energy surface topographies encountered during this process, the ion can fragment through many different conical intersections, transition states, and reaction channels.<sup>44–46</sup> We have shown in many instances<sup>47–50</sup> that the EUV and VUV generated TOFMS can be either nearly identical or different, depending on the molecule and cluster specific orbital cross sections for ionization. Clearly with regard to carbohydrate ionization, these two photon energies can deposit different amounts of energy (associated with different orbital ionizations) into the nascent ion.

Figure 2 presents VUV ionization mass spectra of ribose, the carbohydrate group in RNA, and the previous EUV ionization results<sup>8</sup> for comparison (data in Figure 2(b) are directly adopted from Ref. 8). As in the case of 2-deoxyribose, similar fragment ions are observed, with the VUV radiation leading to less extensive fragmentation and preferentially generating high mass ions. The fragment ions are  $m/z = 60$  ( $C_2H_4O_2^+$ ), 73 ( $C_3H_2O_2^+$ ), 86 ( $C_4H_6O_2^+$ ), 91 ( $C_3H_7O_3^+$ ), 114 ( $C_5H_6O_3^+$ ), 119 ( $C_4H_7O_4^+$ ), and 132 ( $C_5H_8O_4^+$ ). The current results show that the ribose molecule is also very susceptible to bond dissociation and fragmentation near the ionization threshold.

The highly symmetric nature of carbohydrate structures complicates fragment ion identification, and thus fragment channel and fragment mechanism identification, due to mass degeneracies, as shown in Figure 3. For example, in the case of a pentose, at least four possible fragmentation pathways can result in the formation of ions with  $m/z = 60$  ( $C_2H_4O_2^+$ ); assigning the ion to a specific fragment pathway is not possible without additional information. Similar difficulties are also shown in previous studies<sup>8–17</sup> on interactions between high energy particles and 2-deoxyribose, in which the molecular ion undergoes fragmentation and yields ions with various fragmentation pathways involving bond rearrangements, intramolecular proton or hydrogen transfer,

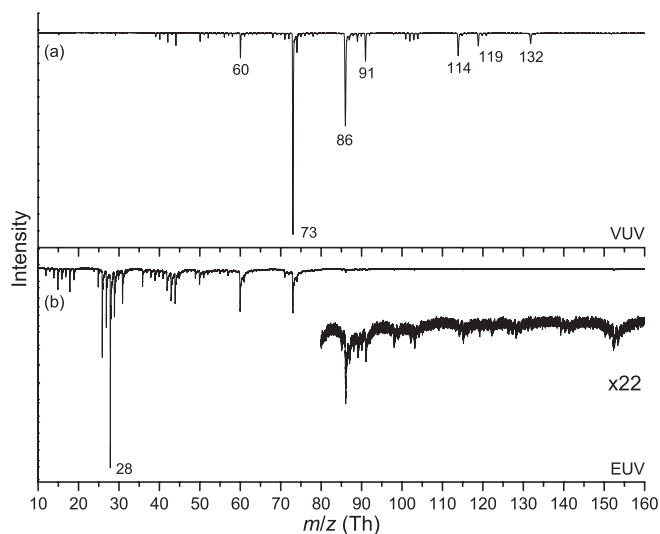


FIG. 2. TOF mass spectra of ribose mixed with a R6G matrix, ionized with (a) VUV and (b) EUV photons. Data presented in (b) are directly adopted from Ref. 8. Similar fragmentation patterns are observed. The molecular ion ( $m/z = 150$ ) is not observed in either case. Reprinted with permission from J.-W. Shin, F. Dong, M. E. Grisham, J. J. Rocca, and E. R. Bernstein, "Extreme ultraviolet photoionization of aldoses and ketoses," *Chem. Phys. Lett.* **506**, 161–166 (2011). Copyright 2011 Elsevier.

and dehydration. While the exact fragmentation pathways remain somewhat ambiguous, suggested<sup>8,9,12,14–17</sup> identities of fragment ions are nearly identical regardless of the ionization method, implying that upon removal of an electron, the molecular ion follows specific relaxation pathways that lead to bond dissociation. For example, dehydration of the 2-deoxyribose molecular ion is observed from other reported ionization studies using VUV,<sup>8,9,15</sup>  $H^+/He^+$ ,<sup>13</sup> and electron<sup>17</sup> sources, and is also observed for ribose in the current study. Similar observations and challenges are presented in Figure 4 for another carbohydrate, xylose. One can infer from inspection of the fragment structures of ribose, xylose, and of 2-deoxyribose the following general ideas: (1) nearly all fragmentation pathways involve endocyclic C–C and C–O bond dissociation and (2) the fragmentation pathways are independent of –OH group orientations and intramolecular hydrogen bonding interactions arising therefrom. The latter point is clear because the C–C and C–O bonds are not involved in the hydrogen bonding network. This is evidenced by the similarity in the two carbohydrate VUV ionization products.

Some of the possible fragmentation pathways can be ruled out by lifting fragment ion mass degeneracies through H, C, or O atom isotopic substitution. Recent isotopic substitution<sup>12</sup> and carbon extraction<sup>16</sup> studies reveal that while nearly all chemical bonds in 2-deoxyribose are prone to dissociation following ionization, certain fragmentation pathways are clearly favored over others. The studies show that chemical bonds at the C5 location most easily undergo dissociation, and complete active space<sup>8</sup> and coupled cluster<sup>9</sup> calculations both support the observation: the C4–C5 bond is most prone to dissociation. VUV ionization mass spectra of xylose (150 amu) and 1,2-<sup>13</sup>C<sub>2</sub>-xylose (152 amu) are

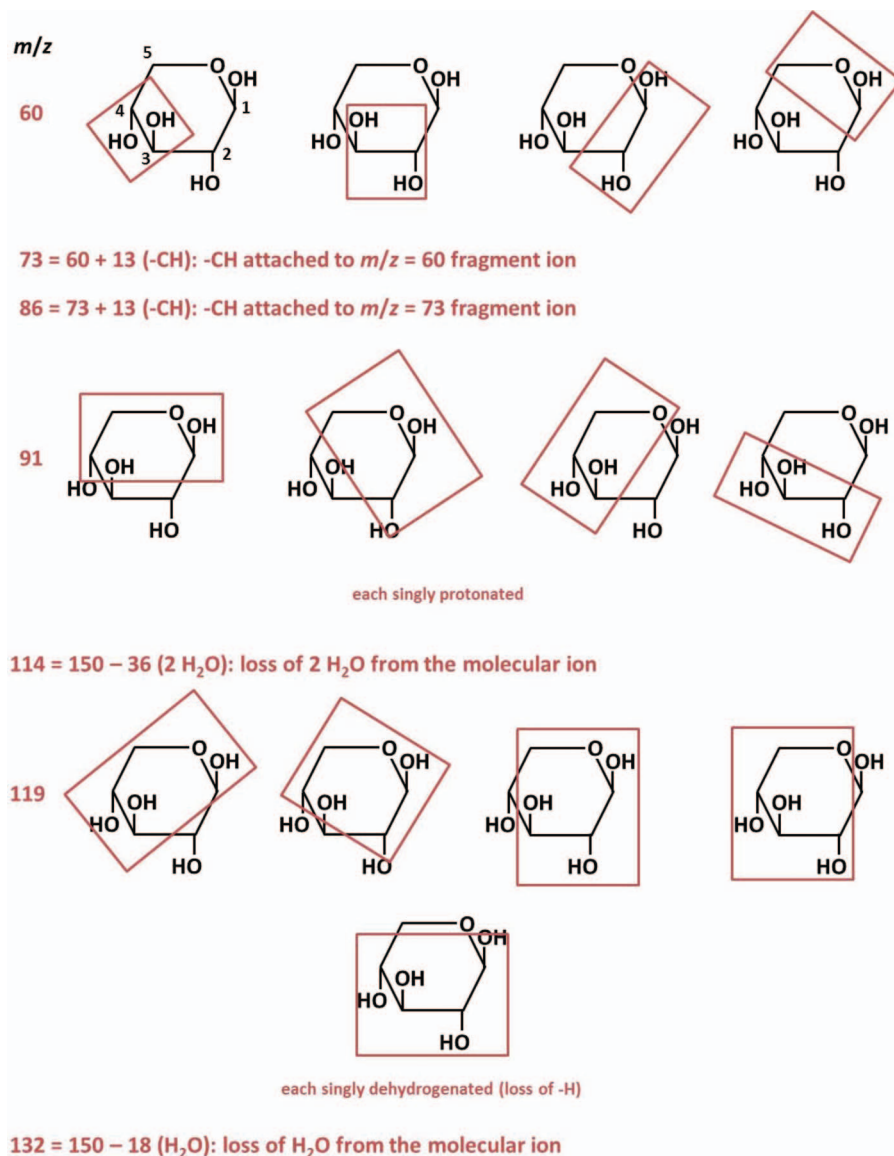


FIG. 3. Haworth projection of xylose showing possible fragmentation sites of pentose ions. H atoms attached to C atoms are omitted for clarity. A Haworth structure with the axial OH group at the C3 position (and other OH groups oriented the same as those in xylose) is ribose.

compared in Figure 4. A shift of  $\Delta(m/z) = 1$  or 2 is observed for all fragment ion peaks; while the double isotopic substitution alone does not unambiguously assign all fragment ions, fragmentation pathways suggested in Figure 5 show that every endocyclic bond is involved in at least one pathway for the generation of major ion peaks, with the exception of the C5-O bond.

DFT calculations are employed to generate an understanding of the reaction channels for ribose and xylose fragmentation. Computational studies suggest that ionization energy calculations performed on DFT optimized structures<sup>51-53</sup> are highly effective in predicting HOMO- $n$  ionization energies, but calculations for MP2 optimized structures<sup>54</sup> are more accurate for HOMO ionization energies. In order to benchmark the two methods, we employ EPT = P3/6-311G(d,p) converged third order pole calculations on X3LYP/6-311G(d,p) and MP2/6-311G(d,p) opti-

mized tetrahydropyran, which constitutes the cyclic backbone of carbohydrates, and compare the results to experimental<sup>55</sup> HOMO and HOMO- $n$  ionization energy values (supplementary material).<sup>56</sup> The comparison shows that the DFT and *ab initio* results are nearly identical, and that both are in excellent agreement with observations. These and previous<sup>51</sup> results are within  $-0.3$ – $0.4$  eV of the experimental<sup>55,57</sup> values. Considering the importance of dispersion interactions in carbohydrates<sup>29</sup> and efficiency of the DFT method as demonstrated above, ribose and xylose are optimized at the X3LYP/6-311G(d,p) level, and ionization energies of several outer valence orbitals are calculated using the P3 method. Results are presented in Figure 6. Taking into account the computational uncertainty, we consider the three orbitals, HOMO, HOMO-1, and HOMO-2, whose ionization energies are around and below 10.9 eV ( $10.49 + 0.4$  eV  $\approx$  10.9 eV; 10.49 eV is the VUV photon energy). One might expect these

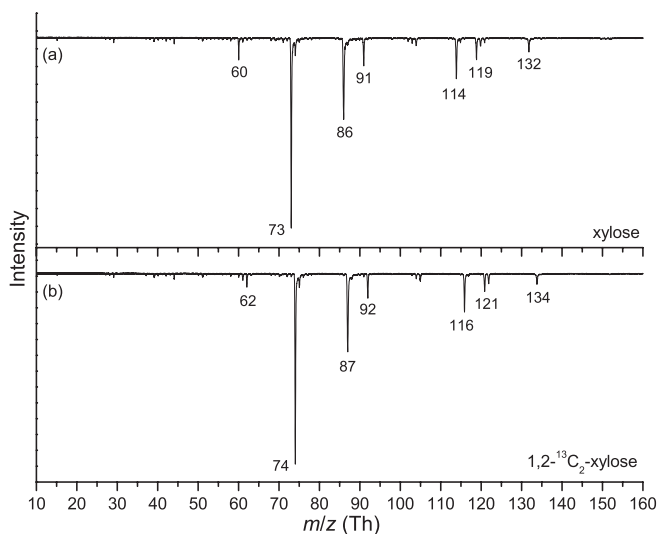


FIG. 4. TOF mass spectra of VUV ionization products of (a) xylose and (b)  $1,2\text{-}^{13}\text{C}_2$ -xylose mixed with R6G.  $\Delta(m/z) = 1$  or 2 is observed for each ion peak.

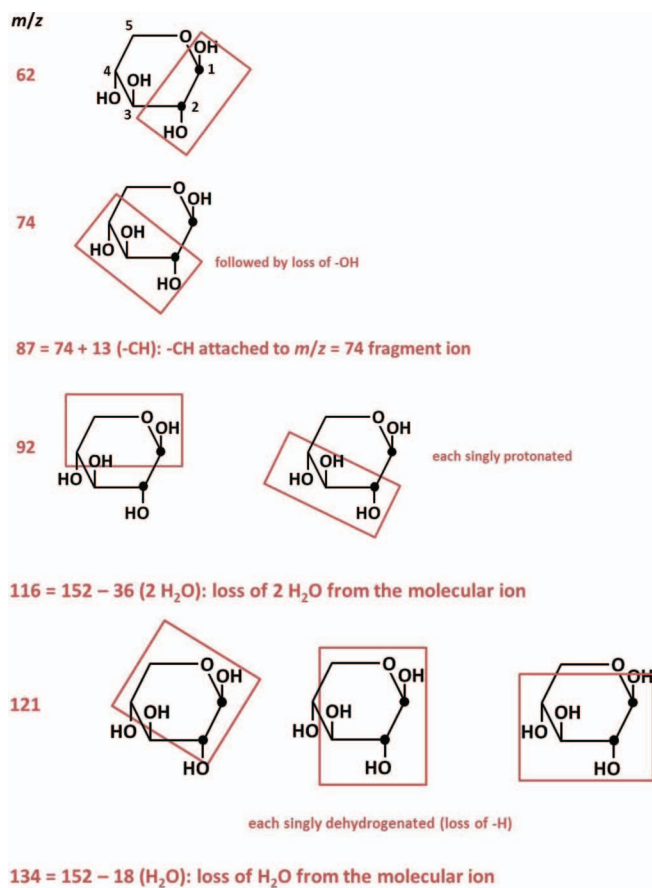


FIG. 5. Haworth projection of xylose showing possible fragmentation sites of pentose ions. The black dots indicate  $^{13}\text{C}$  atoms. H atoms attached to C atoms are omitted for clarity. A Haworth structure with the axial OH group at the C3 position (and other OH groups oriented the same as those in xylose) is ribose.

orbitals to be mostly either on the hydroxyl O or endocyclic O atoms and removal of a nonbonding lone pair electron is the most probable ionization process, but calculations show that the three orbitals are in fact distributed over the entire molecular structure on the endocyclic C–C and C–O bonds with much less significant contribution from the aforementioned hydroxyl O atoms. Thus, as VUV photons remove electrons from C–C and C–O bonds (and not the O atom lone pairs), the bonds become unstable and break, as observed. Note that none of the three molecular orbitals in question locate electron density on the C5–O bond for either ribose or xylose, suggesting that this bond is not accessed by the VUV photons and thereby weakened.

Our finding is consistent with a recent *ab initio* result,<sup>9</sup> which shows that removal of an electron from bonding  $\sigma$  orbitals weakens the endocyclic C–C chemical bonds in 2-deoxyribose and results in molecular ion fragmentation. Our previous<sup>8</sup> study shows that the energy difference between the Franck-Condon ion and adiabatic ion is less than a typical C–C bond strength. This implies<sup>8</sup> that fragmentation of a 2-deoxyribose following ionization is the result of electronic predissociation of the Franck-Condon ion during relaxation to the adiabatic state. Also, the OH group orientation has little effect on the shape and ordering of the endocyclic chemical bonds, which makes the carbohydrate fragmentation pathways independent of the intramolecular hydrogen bonding network.

## B. VUV ionization of nucleotides

As mentioned above, the propensity of carbohydrate ions to fragment has been considered<sup>10–15</sup> as evidence for the idea that radiation damage to DNA and RNA molecules is a consequence of the carbohydrate group undergoing facile fragmentation when exposed to ionizing photons. Since DNA and RNA strand backbones are composed of the carbohydrate molecule linked to nucleobase and phosphate groups, ionization induced carbohydrate fragmentation would certainly lead to nucleic acid radiation damage.

Figure 7 shows VUV ionization mass spectra of nucleotide (sugar, base, and monophosphate) molecules A5MP, C5MP, G5MP, and U5MP, which are the model system building blocks of DNA and RNA. No nucleotide molecular ions are observed, and while a number of ions arising from fragmentation of the carbohydrate and phosphate groups are observed at  $m/z = 42$  ( $\text{C}_2\text{H}_2\text{O}^+$ ), 56 ( $\text{C}_3\text{H}_4\text{O}^+$ ), 68 ( $\text{C}_4\text{H}_4\text{O}^+$ ), 98 ( $\text{PH}_3\text{O}_4^+$ ), and 114 ( $\text{C}_5\text{H}_6\text{O}_3^+$ ), the most prominent feature in the mass spectra is the singly charged intact molecular ions of nucleobases adenine, cytosine, guanine, and uracil at  $m/z = 135$  ( $\text{C}_5\text{H}_5\text{N}_5^+$ ), 111 ( $\text{C}_4\text{H}_5\text{N}_3\text{O}^+$ ), 151 ( $\text{C}_5\text{H}_5\text{N}_5\text{O}^+$ ), and 112 ( $\text{C}_4\text{H}_4\text{N}_2\text{O}_2^+$ ), respectively. Thus, the nucleotides lose both  $\text{PO}_4$  and sugar groups upon ionization. This is an interesting result: the primary fragmentation sites are not in the carbohydrate group that tends to undergo extensive fragmentation, but at the carbohydrate-nucleobase linkage. Similar behavior is found from a low energy electron impact study<sup>58</sup> of solid phase thymidine (deoxyribosylthymine), which generates the nucleobase thymine

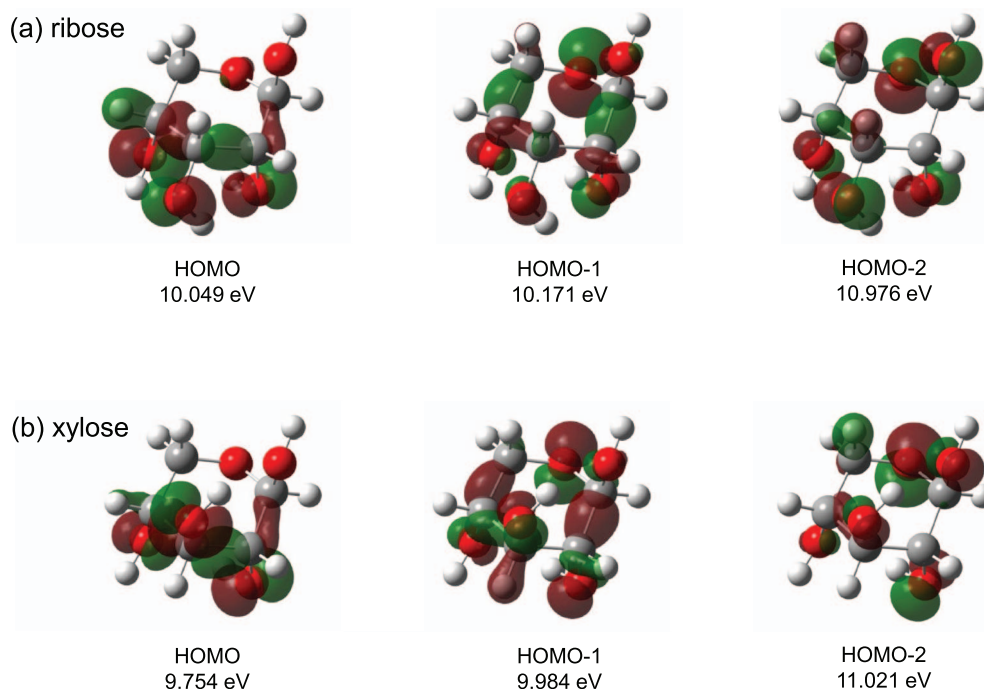


FIG. 6. X3LYP/6-311G(d,p) structures and molecular orbitals of ribose and xylose. The HOMO, HOMO-1, and HOMO-2 are spread over all the chemical bonds, except for the endocyclic C5–O bond. EPT = P3/6-311G(d,p) converged 3rd order pole ionization energies of the orbitals are also shown. HOMO = highest occupied molecular orbital.

following irradiation, and also from a collision activated dissociation study<sup>59</sup> of protonated heterodinucleotide, in which hydrogen transfer to the nucleobase group was observed. The present result implies that direct radiation damage primarily involves formation of stable nucleobase molecular ions through the carbohydrate-nucleobase  $C_{\alpha}$ –N bond dissociation, which is likely accompanied by a hydrogen transfer from the acidic phosphate group to the basic nucleobase N atom.

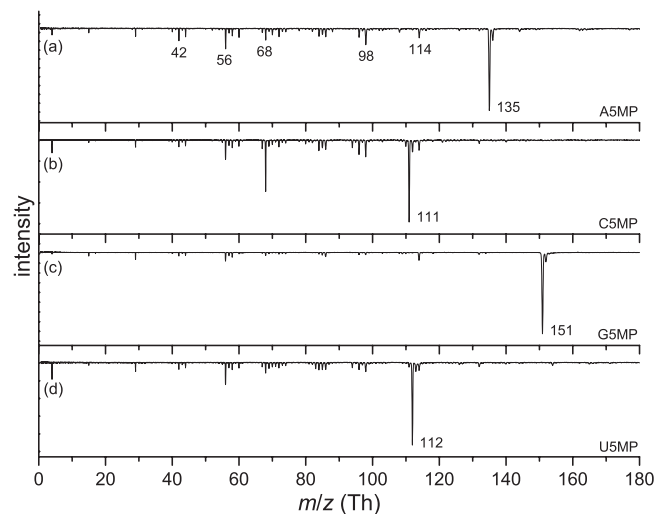


FIG. 7. TOF mass spectra of VUV ionization products of (a) A5MP, (b) C5MP, (c) G5MP, and (d) U5MP mixed with R6G. No nucleotide molecular ions are observed. Ions observed at  $m/z = 135$ , 111, 151, and 112 correspond to nucleobase molecular ions.

Molecular structures and orbitals of the four nucleotides calculated at the X3LYP level are shown in Figure 8. Outer valence orbitals HOMO, HOMO-1, ..., HOMO- $n$  primarily concentrate electron density on the  $\pi$  electron system of the nucleobase group with lesser contribution from the carbohydrate group. The EPT = P3/6-311G(d,p) level of theory can be employed to calculate accurately the ionization energy of each orbital. Application of this method to large molecules, such as the nucleotides, is not practical with our computational resources, however. Considering the current result that fragmentation involving the phosphate group is minimal, and that the P3 ionization energies of phosphoric acid ( $H_3PO_4$ ) exceed 11.5 eV, model systems are used to calculate ionization energies in which the phosphate-methyl ( $H_2PO_4-CH_2$ ) group in each optimized nucleotide structure is replaced with a H atom. The model system structures are not reoptimized to preserve the original carbohydrate and nucleobase parameters.

The next lowest orbital, HOMO- $(n-1)$ , for each species is located on the phosphate group and thus it is not shown in Figure 8. The P3 ionization results show that VUV photons have sufficient energy to ionize any of these nucleobase orbitals. These orbital energy estimates and electron distributions suggest two physical mechanisms for nucleotide fragmentation upon exposure to high energy radiation: (1) ionization of the carbohydrate group is masked due to the presence of the nucleobase group with a lower ionization energy, as evidenced by the weak intensity peaks in the  $m/z = 40$ – $100$  region in the mass spectra and (2) formation of nucleobase molecular ions through the  $C_{\alpha}$ –N bond dissociation involves ionization of the  $\pi$  electron system followed by a H atom transfer.

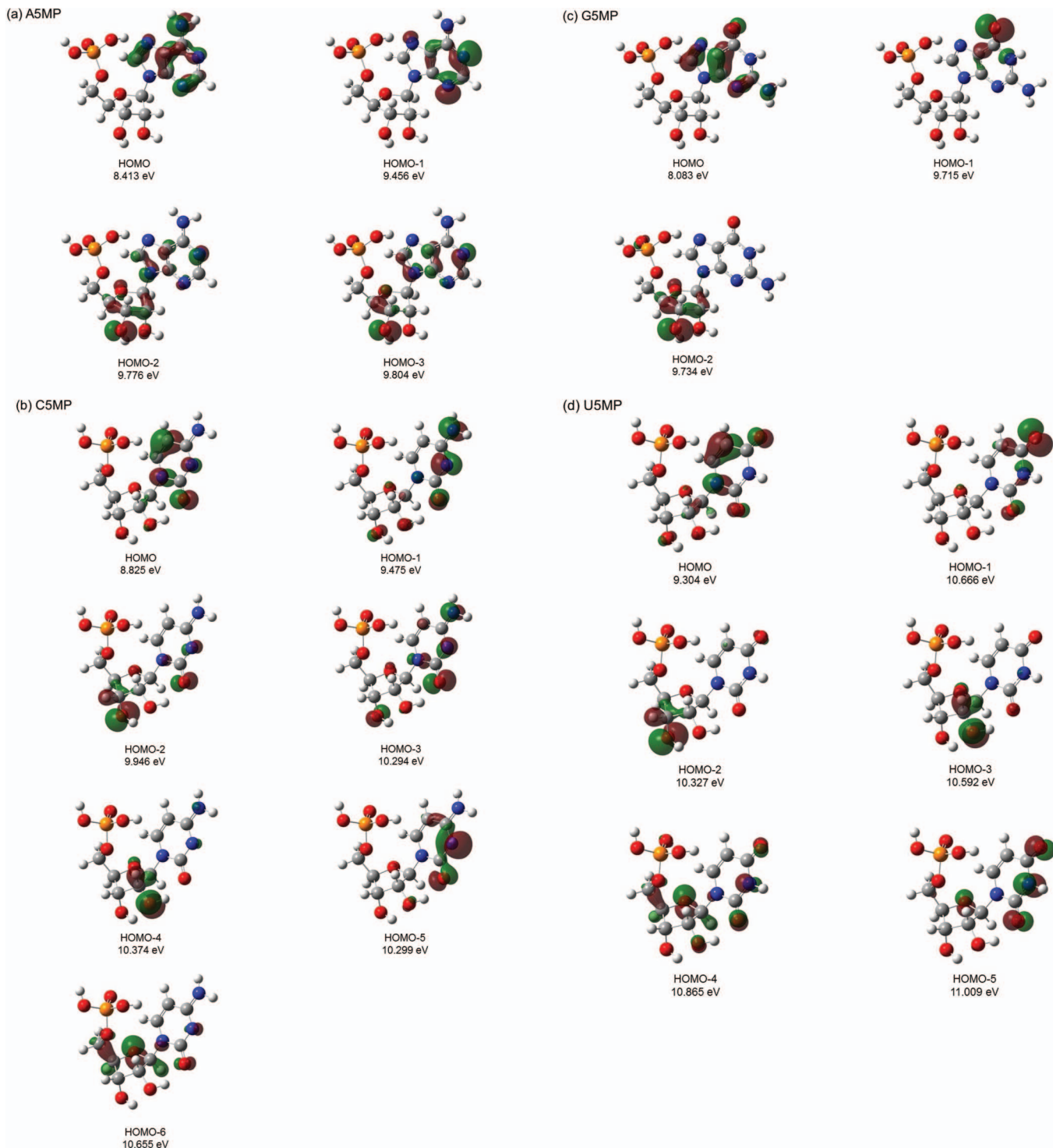


FIG. 8. X3LYP/Gen structures and molecular orbitals of (a) A5MP, (b) C5MP, (c) G5MP, and (d) U5MP. 6-31G is used for C atoms, and 6-31G(d) is used for H, N, O, and P atoms. The ionization energies are calculated at the EPT = P3/6-311G(d,p) level using structures in which the phosphate-methyl ( $\text{H}_2\text{PO}_4\text{-CH}_2$ ) group is replaced with a H atom. The HOMO, HOMO-1, and HOMO-2, . . . , HOMO- $n$  are primarily concentrated on the nucleobase  $\pi$  system. For each nucleotide, the HOMO-( $n-1$ ) (not shown) is located on the phosphate group. HOMO = highest occupied molecular orbital.

## V. CONCLUSIONS

VUV photoionization of chemically unmodified, isolated carbohydrates and nucleotides in the gas phase is accomplished and detected through single photon ionization and time of flight mass spectrometry. Mass analysis shows that all carbohydrates studied undergo extensive fragmentation even

for near threshold ionization, suggesting that their molecular ions are intrinsically unstable. DFT calculations show that the HOMOs and energetically closely lying orbitals are distributed over the entire endocyclic chemical bonding system. These bonds weaken upon ionization and the saccharide molecular ion can readily dissociate. While these results suggest that radiation damage of nucleic acids is related to the

inherent instability of the carbohydrate groups, VUV ionization of nucleotides indicates that the most accessible fragmentation pathway involves the carbohydrate-nucleobase bond dissociation. The current photoionization study and previous low energy electron impact study<sup>58</sup> strongly imply that DNA and RNA damage primarily involves ionization of the nucleobase group followed by phosphate-carbohydrate-nucleobase bond dissociation, and subsequent fragmentation of the carbohydrate group. Under VUV irradiation, neutral nucleotides and protonated oligonucleotides<sup>33</sup> fragment by very different mechanisms and into different components of the carbohydrate and phosphate moieties: nonetheless, they both generate stable nucleobase moieties.

A true sense of the dynamics and the mechanisms of these excitation, ionization, and fragmentation processes must rely on more sophisticated and comprehensive multi-reference calculations (e.g., CASSCF and CASPT2), non-Born Oppenheimer interactions between the many potential energy surfaces involved, and a thorough search for conical intersections coupling these various processes.

## ACKNOWLEDGMENTS

E.R.B. and J.W.S. acknowledge support from the US Army Research Office (FA9550-10-1-0454), the National Science Foundation (NSF) Engineering Research Center for Extreme Ultraviolet Science and Technology (0310717), and the NSF through the Extreme Science and Engineering Discovery Environment supercomputer resources provided by San Diego Supercomputer Center (TG-CHE110083). J.W.S. also acknowledges support from the NSF through the Extreme Science and Engineering Discovery Environment supercomputer resources provided by Pittsburgh Supercomputing Center (TG-CHE130050) and the Division of Science at Governors State University.

- <sup>1</sup>H.-W. Jochims, M. Schwell, H. Baumgärtel, and S. Leach, *Chem. Phys.* **314**, 263 (2005).
- <sup>2</sup>K.-W. Choi, D.-S. Ahn, J.-H. Lee, and S. K. Kim, *Chem. Comm.* **2007**, 1041.
- <sup>3</sup>Y. Hu and E. R. Bernstein, *J. Chem. Phys.* **128**, 164311 (2008).
- <sup>4</sup>L. Zhang, Y. Pan, H. Guo, T. Zhang, L. Sheng, F. Qi, P.-K. Lo, and K.-C. Lau, *J. Phys. Chem. A* **113**, 5838 (2009).
- <sup>5</sup>Y. Pan, L. Zhang, T. Zhang, H. Guo, X. Hong, L. Sheng, and F. Qi, *Phys. Chem. Chem. Phys.* **11**, 1189 (2009).
- <sup>6</sup>H. Guo, L. Zhang, L. Deng, L. Jia, Y. Pan, and F. Qi, *J. Phys. Chem. A* **114**, 3411 (2010).
- <sup>7</sup>G. L. Gasper, L. K. Takahashi, J. Zhou, M. Ahmed, J. F. Moore, and L. Hanley, *Anal. Chem.* **82**, 7472 (2010).
- <sup>8</sup>J.-W. Shin, F. Dong, M. Grisham, J. J. Rocca, and E. R. Bernstein, *Chem. Phys. Lett.* **506**, 161 (2011).
- <sup>9</sup>D. Ghosh, A. Golan, L. K. Takahashi, A. I. Krylov, and M. Ahmed, *J. Phys. Chem. Lett.* **3**, 97 (2012).
- <sup>10</sup>K. Fujii, K. Akamatsu, and A. Yokoya, *Surf. Sci.* **528**, 249 (2003).
- <sup>11</sup>Z. Deng, I. Bald, E. Illenberger, and M. A. Huels, *Phys. Rev. Lett.* **95**, 153201 (2005).
- <sup>12</sup>I. Bald, Z. Deng, E. Illenberger, and M. A. Huels, *Phys. Chem. Chem. Phys.* **8**, 1215 (2006).
- <sup>13</sup>F. Alvarado, S. Bari, R. Hoekstra, and T. Schlathöler, *Phys. Chem. Chem. Phys.* **8**, 1922 (2006).
- <sup>14</sup>Z. Deng, I. Bald, E. Illenberger, and M. A. Huels, *J. Chem. Phys.* **127**, 144715 (2007).
- <sup>15</sup>G. Vall-Iosera, M. A. Huels, M. Coreno, A. Kivimäki, K. Jakubowska, M. Stankiewicz, and E. Rachlew, *ChemPhysChem* **9**, 1020 (2008).
- <sup>16</sup>Z. Deng, I. Bald, E. Illenberger, and M. A. Huels, *Angew. Chem., Int. Ed.* **47**, 9509 (2008).
- <sup>17</sup>S. Ptasíńska, S. Deniff, P. Scheier, and T. P. Märk, *J. Chem. Phys.* **120**, 8505 (2004).
- <sup>18</sup>J. R. Srinivasan, L. J. Romano, and R. J. Levis, *J. Phys. Chem.* **99**, 13272 (1995).
- <sup>19</sup>A. Bhattacharya, Y. Q. Guo, and E. R. Bernstein, *J. Phys. Chem. A* **113**, 811 (2009).
- <sup>20</sup>Y. Q. Guo, A. Bhattacharya, and E. R. Bernstein, *J. Chem. Phys.* **134**, 024318 (2011).
- <sup>21</sup>Y. Q. Guo, A. Bhattacharya, and E. R. Bernstein, *J. Chem. Phys.* **128**, 034303 (2008).
- <sup>22</sup>M. Greenfield, Y. Q. Guo, and E. R. Bernstein, *Chem. Phys. Lett.* **430**, 277 (2006).
- <sup>23</sup>M. Staniforth and V. G. Stavros, *Proc. R. Soc. London, Ser. A* **469**, 20130458 (2013).
- <sup>24</sup>J.-W. Shin and E. R. Bernstein, *J. Chem. Phys.* **130**, 214306 (2009).
- <sup>25</sup>Y. J. Shi, S. Consta, A. K. Das, B. Mallik, D. Lacey, and R. H. Lipson, *J. Chem. Phys.* **116**, 6990 (2002).
- <sup>26</sup>Y. J. Hu, H. B. Fu, and E. R. Bernstein, *J. Chem. Phys.* **125**, 154306 (2006).
- <sup>27</sup>Y. J. Hu, H. B. Fu, and E. R. Bernstein, *J. Chem. Phys.* **125**, 184308 (2006).
- <sup>28</sup>M. J. Frisch, G. W. Trucks, H. B. Schlegel *et al.*, GAUSSIAN 09, Revision C.01, Gaussian, Inc., Wallingford, CT, 2009.
- <sup>29</sup>E. J. Cocinero, A. Lesarri, P. Écija, Á. Cimas, B. G. Davis, F. J. Basterretxea, J. A. Fernández, and F. Castaño, *J. Am. Chem. Soc.* **135**, 2845 (2013).
- <sup>30</sup>X. Xu and W. A. Goddard III, *Proc. Natl. Acad. Sci. U.S.A.* **101**, 2673 (2004).
- <sup>31</sup>J. V. Ortiz, *J. Chem. Phys.* **104**, 7599 (1996).
- <sup>32</sup>J. V. Ortiz and V. G. Zakrzewski, *J. Chem. Phys.* **105**, 2762 (1996).
- <sup>33</sup>O. González-Magaña, M. Tiemens, G. Reitsma, L. Boschman, M. Door, S. Bari, P. O. Lahaie, J. R. Wagner, M. A. Huels, R. Hoekstra, and T. Schlathöler, *Phys. Rev. A* **87**, 032702 (2013).
- <sup>34</sup>H. Guo, L. Zhang, L. Deng, L. Jia, Y. Pan, and F. Qi, *J. Phys. Chem. A* **114**, 3411 (2010).
- <sup>35</sup>S. Pilling, A. F. Lago, L. H. Coutinho, R. B. de Castilho, G. G. B. de Souza, and A. N. de Brito, *Rapid Commun. Mass Spectrom.* **21**, 3646 (2007).
- <sup>36</sup>O. Plekan, V. Feyer, R. Richter, M. Coreno, M. de Simone, K. C. Prince, and V. Carravetta, *J. Phys. Chem. A* **111**, 10998 (2007).
- <sup>37</sup>M. Geronés, M. F. Erben, R. M. Romano, and C. O. D. Védova, *J. Phys. Chem. A* **112**, 2228 (2008).
- <sup>38</sup>M. Geronés, A. J. Downs, M. F. Erben, M. Ge, R. M. Romano, L. Yao, and C. O. D. Védova, *J. Phys. Chem. A* **112**, 5947 (2008).
- <sup>39</sup>O. Plekan, M. Coreno, V. Feyer, A. Moise, R. Richter, M. de Simone, R. Sankari, and K. C. Prince, *Phys. Scr.* **78**, 058105 (2008).
- <sup>40</sup>V. Feyer, O. Plekan, R. Richter, M. Coreno, and K. C. Prince, *Chem. Phys.* **358**, 33 (2009).
- <sup>41</sup>M. Klessinger and J. Michl, *Excited States and Photochemistry of Organic Molecules* (VCH Publishers, Inc., New York, 1995), pp. 179–192.
- <sup>42</sup>N. J. Turro, V. Ramamurthy, and J. C. Scaiano, *Modern Molecular Photochemistry of Organic Molecules* (University Science Books, Sausalito, CA, 2010), pp. 319–382.
- <sup>43</sup>A. Bhattacharya, Y. Q. Guo, and E. R. Bernstein, *Acc. Chem. Res.* **43**, 1476 (2010).
- <sup>44</sup>A. Bhattacharya, J.-W. Shin, K. J. Clawson, and E. R. Bernstein, *Phys. Chem. Chem. Phys.* **12**, 9700 (2010).
- <sup>45</sup>Y. Q. Guo, A. Bhattacharya, and E. R. Bernstein, *J. Phys. Chem. A* **115**, 9349 (2011).
- <sup>46</sup>Z. Yu and E. R. Bernstein, *J. Phys. Chem. A* **117**, 1756 (2013).
- <sup>47</sup>F. Dong, S. Heinbuch, Y. Xie, J. J. Rocca, and E. R. Bernstein, *J. Am. Chem. Soc.* **130**, 1932 (2008).
- <sup>48</sup>S.-G. He, Y. Xie, F. Dong, S. Heinbuch, E. Jakubikova, J. J. Rocca, and E. R. Bernstein, *J. Phys. Chem. A* **112**, 11067 (2008).
- <sup>49</sup>F. Dong, S. Heinbuch, Y. Xie, J. J. Rocca, and E. R. Bernstein, *J. Phys. Chem. A* **113**, 3029 (2009).
- <sup>50</sup>F. Dong, S. Heinbuch, Y. Xie, J. J. Rocca, and E. R. Bernstein, *Phys. Chem. Chem. Phys.* **12**, 2569 (2010).
- <sup>51</sup>B. Herrera, O. Dolgounitcheva, V. G. Zakrzewski, A. Toro-Labbé, and J. V. Ortiz, *J. Phys. Chem. A* **108**, 11703 (2004).
- <sup>52</sup>C. T. Falzon and F. Wang, *J. Chem. Phys.* **123**, 214307 (2005).
- <sup>53</sup>W. Adcock, M. J. Brunger, I. E. McCarthy, M. T. Michalewicz, W. von Niessen, F. Wang, E. Weigold, and D. A. Winkler, *J. Am. Chem. Soc.* **122**, 3892 (2000).

<sup>54</sup>D. M. Close, *J. Phys. Chem. A* **115**, 2900 (2011).

<sup>55</sup>A. A. Planckaert, J. Doucet, and C. Sandorfy, *J. Chem. Phys.* **60**, 4846 (1974).

<sup>56</sup>See supplementary material at <http://dx.doi.org/10.1063/1.4862829> for comparison of experimental and computational ionization energies of tetrahydropyran.

<sup>57</sup>T. P. Debies and J. W. Rabalais, *J. Electron. Spectrosc. Relat. Phenom.* **3**, 315 (1974).

<sup>58</sup>Y. Zheng, P. Cloutier, D. J. Hunting, J. R. Wagner, and L. Sanche, *J. Am. Chem. Soc.* **126**, 1002 (2004).

<sup>59</sup>D. R. Phillips and J. A. McCloskey, *Int. J. Mass Spectrom. Ion Processes* **128**, 61 (1993).